Improved Edge Charge Exchange Recombination Spectroscopy in DIII-D[a)]

C. Chrystal,[1, b)] K. H. Burrell,[2] B. A. Grierson,[3] S. R. Haskey,[3] R. J. Groebner,[2] D. H. Kaplan,[2] and A. Briesemeister[4]

[1)] *Oak Ridge Associated Universities, Oak Ridge, Tennessee 37831, USA*
[2)] *General Atomics, PO Box 85608, San Diego, California 92186-5608, USA*
[3)] *Princeton Plasma Physics Laboratory, Princeton, New Jersey 08543-0451, USA*
[4)] *Oak Ridge National Laboratory, Oak Ridge, Tennessee 37831, USA*

(Dated: 19 June 2016)

The charge exchange recombination spectroscopy diagnostic on the DIII-D tokamak has been upgraded with the addition of more high radial resolution view chords near the edge of the plasma ($r/a > 0.8$). The additional views are diagnosed with the same number of spectrometers by placing fiber optics side-by-side at the spectrometer entrance with a precise separation that avoids wavelength shifted crosstalk without the use of bandpass filters. The new views improve measurement of edge impurity parameters in steep gradient, H-mode plasmas with many different shapes. The number of edge view chords with 8 mm radial separation has increased from 16 to 38. New fused silica fibers have improved light throughput and clarify the observation of non-Gaussian spectra that suggest the ion distribution function can be non-Maxwellian in low collisionality plasmas.

I. INTRODUCTION

Charge exchange recombination spectroscopy[1] (CER) is a common diagnostic technique that measures ion temperature, rotation, and density in tokamak plasmas. CER has been used on the DIII-D tokamak since its creation[2] and has undergone numerous upgrades since then[3–9]. This paper details the most recent upgrade to the impurity CER system: an expansion of edge high spatial resolution measurements. Since their original installation, the high spatial resolution edge vertical and tangential measurements have been instrumental for studying the fine structure of the H-mode pedestal and the associated radial electric field well[10]. The radial electric field is a key aspect of current studies of pedestal confinement in tokamak fusion.

The location of the original high resolution edge measurements was suboptimal for some plasma shapes that employ relatively large gaps between the outer wall and the last closed flux surface (usually to reduce the heat load on limiting surfaces). Detailed edge measurements could be recovered in these plasmas by slowly scanning the major radius of the plasma edge, but this greatly reduced the effective time resolution. The addition of more high resolution views eliminates this limitation. Adding view chords can require significant resources when additional spectrometers are required. This upgrade was enabled by a new optical configuration that increased the number of measurements made with existing spectrometers.

[a)] Contributed paper published as part of the Proceedings of the 21st Topical Conference on High-Temperature Plasma Diagnostics, Madison, Wisconsin, June, 2016.

[b)] Author to whom correspondence should be addressed: chrystal@fusion.gat.com

II. CONFIGURATION AND RESULTS

The upgraded impurity CER system on DIII-D has 80 view chords. 38 are concentrated near the outboard midplane of the tokamak, half viewing tangentially and half viewing vertically. Adjacent view chords of the same type are ≈ 8 mm apart in major radius and radial coverage is from 2.18 to 2.32 m. This enables measurement from the top of the pedestal to the scrape off layer for all but the most exotic DIII-D shapes. Previously, 22 view chords covered this same region, and only 16 had ≈ 8 mm separation. A cross section view of the current system is shown in Fig. 1.

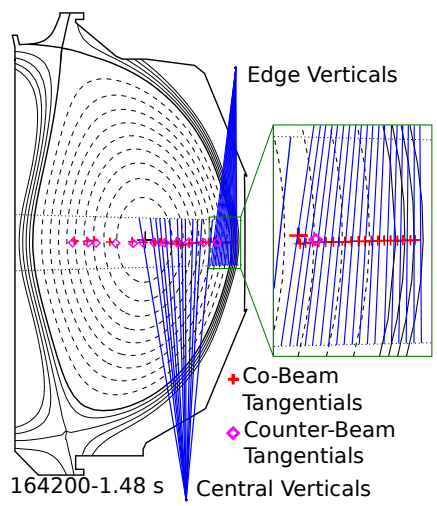

FIG. 1. A cross section view of DIII-D and its CER view chords. The inset details the expanded edge coverage.

The upgraded edge view chords use previously existing port optics and new fused silica fiber optics. The fibers consist of two 0.75 mm core diameter fibers whose tips are contained in a compact, rigid aluminum case. This

allows the fibers to be closely packed in order to achieve maximum radial resolution. In the plasma, the two fiber cores are imaged on top of one another for tangential view chords and toroidally displaced from one another for vertical view chords. These orientations exploit the symmetry of the plasma to increase the acquired signal without decreasing radial resolution. The previous fibers were installed over 20 years ago and had suffered significant radiation browning, so the new fibers have $\approx 3\times$ more light throughput. This fiber installation was performed in conjunction with an upgrade to the main-ion CER system[11].

Minor hardware modifications allowed six of the new view chords to be integrated into existing spectrometer and camera systems. The other 32 view chords are imaged with the same four spectrometers that previously imaged 16 view chords. This was accomplished with two, side-by-side slits and using new CCD detectors that are wide enough to image both slits. Each scanning 2/3 m Czerny-Turner spectrometer uses 1400 g/mm gratings and images eight view chords on two SRI Avanti-768 CCD detectors. These detectors have a chip size of 768×256 pixels with 18 μm square pixels. The dispersion is ≈ 9 pixels/Å.

No bandpass filters are used to prevent wavelength shifted crosstalk between fibers mounted on side-by-side slits. The wavelength shift was designed to be 62 Å when viewing the standard C-VI emission ($n = 8 \rightarrow 7$, 5291 Å). No harmful crosstalk is observed with this separation. This is true whether or not modulated beams are used to subtract the passive portion of the spectrum. Similar side-by-side spectra were analyzed at TCV with modulated beams[12], and tests on DIII-D were performed before this upgrade to determine the proper wavelength shift. These tests were done during standard DIII-D discharges, so it is possible that when non-standard impurities are present, previously unobserved crosstalk will occur. To date, deliberate introduction of argon, boron, chlorine, fluorine, lithium, neon, and nitrogen has not contaminated the standard C-VI emission. In addition, no significant crosstalk has been found when the edge CER system has been tuned to observe the B-V ($n = 7 \rightarrow 6$, 4945 Å), Ne-X ($n = 11 \rightarrow 10$, 5248 Å), N-VII ($n = 9 \rightarrow 8$, 5669 Å), and Li-III ($n = 7 \rightarrow 5$, 5167 Å) charge exchange emission.

If significant crosstalk is encountered, either slit on each spectrometer can be blocked via remote control of push-pull solenoids that move a thin piece of black anodized aluminum into the optical path of either slit. This eliminates any chance of cross talk while decreasing radial resolution. These slit blockers are routinely employed during intensity and wavelength calibrations[13].

One of the first experiments performed on DIII-D after the upgraded edge CER system became available had a relatively low major radius pedestal. The upgraded system makes much better measurements in the edge of this plasma than the previous system would have. Two of the measurements that can be made by CER are shown in Fig. 2 to demonstrate the improvement.

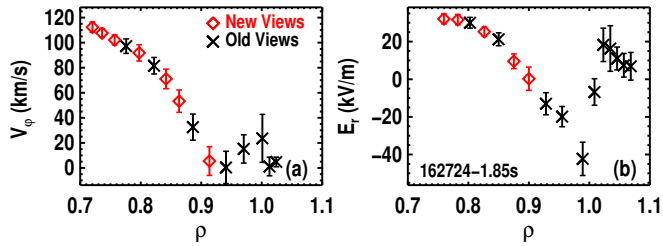

FIG. 2. Edge profiles of (a) toroidal rotation and (b) radial electric field measured by the upgraded edge CER system as a function of ρ, the normalized toroidal flux. New views add significant spatial resolution. Note that several views are not shown because they are deep in the scrape off layer.

The increased signal of edge chords has clarified the observation of non-Gaussian spectra, an example of which is shown in Fig. 3. The presence of these spectra is observed to have a complex dependence on position and plasma conditions, so a simple measurement artifact (e.g. fine structure, passive emission, etc.) is an unlikely explanation. For now, these spectra are treated as an observation of non-Maxwellian emission. The root cause of this is of great interest. One possible explanation is that spatial averaging over the observed volume yields a non-Maxwellian spectrum even though the local distribution functions are Maxwellian. This mechanism would yield increased non-Gaussian features when the gradient scale lengths decrease. Another possible explanation is that low collisionality, in conjunction with significant gradients, allows banana orbits to persist such that any local volume contains a significant number of particles executing orbits centered at a different position, and the local distribution function is inherently non-Maxwellian because the plasma is not locally equilibrated[14].

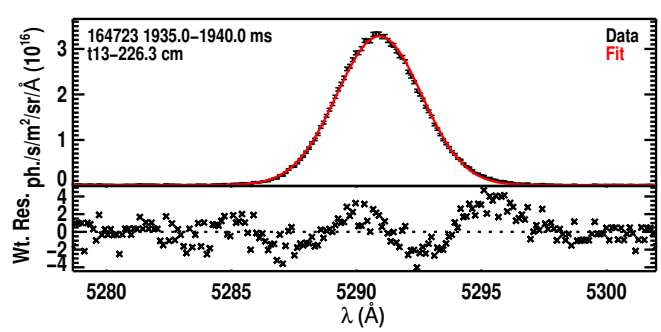

FIG. 3. Example edge CER spectrum that is not well fit by a Maxwellian distribution function. Residuals are weighted by the inverse square of the measurement uncertainty.

To recover the standard measurements from non-Gaussian spectra, a more complex fit model that combines two (or more) Maxwellian distribution functions is used. The amplitude, location, and width of these two distributions differ and yield a fit with flat residuals.

This result fulfills the primary goal of creating an analytic model for the distribution function. The intensity, velocity, and temperature of this distribution function are found by taking moments in the standard way. These results have systematic differences from the simple result produced when using only a single Maxwellian. For instance, when using two Maxwellian distributions to fit the result in Fig. 3, differences of 40 eV and 1.4 km/s are found (error in intensity is negligible). These differences are less than 10% and, in absolute terms, approaching the underlying measurement accuracy. This level of error is typical for views that observe the strongest non-Gaussian features. These views are in the steep-gradient region of the pedestal.

To investigate the cause of these non-Gaussian spectra, it is necessary to create a metric for the strength of this effect. The metric chosen is formed from the FFT of the residuals in a region around the charge-exchange peak by calculating the ratio between the power at long and short wavelengths. The ideal residuals resemble white noise, but spectra like the one seen in Fig. 3 show significant long wavelength components, resulting in much higher metrics (larger ratios). The region analyzed is based on the width of the fit, and the cutoff from long to short wavelengths corresponds to a $n = 6$ standing wave in the chosen region (no shorter wavelength residual patterns have been observed).

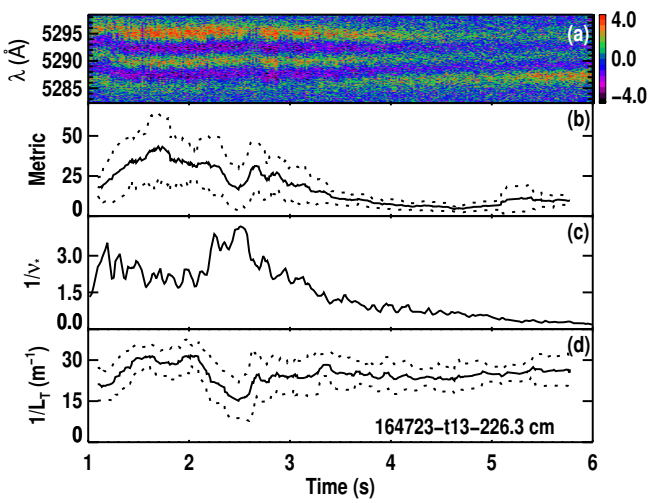

FIG. 4. (a) Weighted residuals of a single Gaussian fit to charge-exchange emission, (b) non-Gaussian metric, (c) collisionality, and (d) temperature gradient scale length for a view chord near the top of the pedestal in a discharge with a significant density ramp.

This metric was used to investigate the non-Gaussian emission near the top of the pedestal during a large density ramp, as seen in Fig. 4. The non-Gaussian nature is initially strong but weakens as collisionality (ν_*) rises while the temperature gradient scale length ($L_T \equiv T/\nabla T$) is nearly constant. ν_* determines the extent that finite orbit width effects are present while spatial averaging is only sensitive to the plasma gradients (L_T is a proxy). This result strongly suggests that an orbit width effect, as opposed to spatial averaging, is the more likely explanation of the non-Gaussian spectra. The correlation coefficient between the non-Gaussian metric and $1/\nu_*$ is 0.50 while it is only 0.36 with $1/L_T$.

Further investigations with a pair of discharges (164629 and 164708) that scanned only collisionality[15,16] found a 4× increase in the non-Gaussian metric concurrent with a 7× increase in $1/\nu_*$ ($1/L_T$, β, ρ_*, etc. were constant). It is also observed that the non-Gaussian metric is larger for tangential view chords than for vertical view chords (≈ 1.5× for the discharge shown in Fig. 4) while the observed volume is about half as large. These results are expected from an orbit width perspective and unexpected from a spatial averaging perspective. Non-Gaussian features are weaker, but not absent, for vertical view chords, making plume emission an unlikely explanation.

ACKNOWLEDGMENTS

This material is based upon work supported by the U.S. Department of Energy, Office of Science, Office of Fusion Energy Sciences, using the DIII-D National Fusion Facility, a DOE Office of Science user facility, under Award DE-FC02-04ER54698, DE-AC02-09CH11466, and DE-AC05-00OR22725. DIII-D data shown in this paper can be obtained in digital format by following the links at https://fusion.gat.com/global/D3D_DMP.

[1] R. Isler, Plasma Phys. Controlled Fusion **36**, 171 (1994).
[2] R. Seraydarian, K. H. Burrell, N. Brooks, R. Groebner, and C. Kahn, Rev. Sci. Instrum. **57**, 155 (1986).
[3] R. P. Seraydarian, K. H. Burrell, and R. J. Groebner, Rev. Sci. Instrum. **59**, 1530 (1988).
[4] P. Gohil, K. H. Burrell, R. J. Groebner, and R. P. Seraydarian, Rev. Sci. Instrum. **61**, 2949 (1990).
[5] D. M. Thomas, K. H. Burrell, R. J. Groebner, P. Gohil, D. Kaplan, C. Makariou, and R. P. Seraydarian, Rev. Sci. Instrum. **68**, 1233 (1997).
[6] K. H. Burrell, D. H. Kaplan, P. Gohil, D. G. Nilson, R. J. Groebner, and D. M. Thomas, Rev. Sci. Instrum. **72**, 1028 (2001).
[7] K. H. Burrell, P. Gohil, R. Groebner, D. Kaplan, J. Robinson, and W. Solomon, Rev. Sci. Instrum. **75**, 3455 (2004).
[8] W. M. Solomon, K. H. Burrell, R. Feder, A. Nagy, P. Gohil, and R. J. Groebner, Rev. Sci. Instrum. **79**, 10F531 (2008).
[9] C. Chrystal, K. H. Burrell, B. Grierson, R. Groebner, and D. Kaplan, Rev. Sci. Instrum. **83**, 10D501 (2012).
[10] R. Groebner, K. H. Burrell, P. Gohil, and R. Seraydarian, Rev. Sci. Instrum. **61**, 2920 (1990).
[11] B. A. Grierson, K. H. Burrell, C. Chrystal, R. J. Groebner, S. R. Haskey, and D. H. Kaplan, Rev. Sci. Instrum. (submitted).
[12] A. Bortolon, *Plasma Rotation and Momentum Transport Studies in the TCV Tokamak Based on Charge Exchange Spectroscopy Measurements*, Ph.D. Thesis, École Polytechnique Fédérale de Lausanne (2009).
[13] P. Gohil, K. H. Burrell, R. J. Groebner, K. Holtrop, D. H. Kaplan, and P. Monier-Garbet, Rev. Sci. Instrum. **70**, 878 (1999).
[14] D. J. Battaglia, K. H. Burrell, C. S. Chang, S. Ku, J. S. Degrassie, and B. A. Grierson, Phys. Plasmas **21**, 072508 (2014).
[15] C. Petty, Phys. Plasmas **15**, 080501 (2008).
[16] T. C. Luce, C. C. Petty, and J. G. Cordey, Plasma Phys. Controlled Fusion **50**, 043001 (2008).